

# Evaluating the consistency between prescriptive and performance-based seismic design approaches for reinforced concrete moment frame buildings



Siamak Sattar

National Institute of Standards and Technology, Gaithersburg, MD, United States

## ABSTRACT

The performance of 4- and 8-story reinforced concrete (RC) moment frame buildings designed in accordance with ASCE/SEI 7–10 is assessed using ASCE/SEI 41. Practicing engineers are increasingly using ASCE/SEI 41 as the standard to implement performance-based seismic design and to demonstrate the adequacy of the seismic performance of new buildings. However, ASCE/SEI 41 was originally developed to assess the structural performance of existing buildings. On the other hand, ASCE 7 is a prescriptive standard that has been used for the design of new buildings for several decades. The correlation between the target performance of the ASCE/SEI 41- and ASCE 7-code compliant buildings is unknown for RC moment frames. In order to compare the anticipated structural performance between ASCE/SEI 7 and ASCE/SEI 41, the seismic performance of 4- and 8-story ASCE/SEI 7 code-compliant special reinforced concrete moment frame buildings is assessed based on the four evaluation methodologies defined in the Tier 3 analysis of ASCE/SEI 41 for the collapse prevention and life safety performance levels. The evaluation results show that depending on the ASCE/SEI 41 evaluation approach employed, the buildings designed per ASCE/SEI 7 may not meet the expected performance in ASCE/SEI 41 and need to be retrofitted.

## 1. Introduction

Since 1990s, following the lessons learned from the 1989 Loma Prieta and Northridge earthquakes, an interest has grown in the U.S. to implement performance-based seismic engineering (PBSE) for the design of buildings. A study conducted by the Applied Technology Council (ATC), and funded by the Federal Emergency Management Agency (FEMA), under the ATC-33 project, was the first effort toward codifying PBSE for implementation in practice for existing buildings. The main output of this project was FEMA 273 [1]. Three years later in 2000, FEMA and ASCE updated FEMA 356 [2] to change it into a national pre-standard, and published FEMA 356 [2]. In 2006, American Society of Civil Engineers (ASCE) published ASCE/SEI 41-06 [3] as the standard for applying the PBSE concepts in seismic rehabilitation of existing buildings. ASCE/SEI 41-13 [4], hereafter referred to as ASCE 41, is employed in this study. In recent years, structural engineers have increasingly employed PBSE as a philosophy for the design of new buildings because of the capability of this approach in quantifying the response of the building against an explicit target performance that is not feasible under traditional prescriptive design standards [5]. As such, ASCE 41 has been employed in the design of new buildings, and is widely considered as a “first generation” performance-based seismic design (PBSD) approach [6]. For instance, ASCE 41 has been adopted in many west coast jurisdictions and has been prescribed by the General Services Administration (GSA) to be used for computing the modeling parameters and acceptance criteria used in the seismic design of new

federal facilities in PBS 100 [7]. Moreover, Chapter 16 of ASCE 7-16 refers to ASCE 41 for modeling and acceptance criteria of components in the seismic force resisting systems. Despite the increasing interest in PBSD in recent years, ASCE/SEI 7-10 [8], hereafter referred to as ASCE 7, remains the standard developed for computing the design loads for new buildings in the U.S.

Considering the available standards used for defining the loads, modeling, or acceptance criteria used in the design and evaluation of buildings, a challenging issue is whether these standards (ASCE 7 and ASCE 41) provide consistent structural performance. A few studies have been conducted in recent years to investigate the correlation between the expected performance in ASCE 41 and ASCE 7. Hagen [9] assessed the performance of a ASCE 7-05 code-compliant 6-story special RC shear wall building using ASCE 41-06, and showed that the building met the Basic Safety Objective in accordance with ASCE 41-06. Speicher and Harris [10,11] and Harris and Speicher [6] assessed the seismic performance of ASCE 7-10 code-compliant buildings per ASCE 41 for three steel structural systems including eccentrically braced frames, special concentrically braced frames and special moment frames. The authors found that the new buildings designed per requirements in ASCE 7 do not meet the seismic performance target expected by ASCE 41-06 for the Basic Safety Objective.

This study investigates the correlation between the performance targeted by ASCE 41 and ASCE 7 for RC moment frames. A set of 4- and 8-story reinforced concrete special moment frames (SMFs) are designed in accordance with ASCE 7 and evaluated using the four different

E-mail address: [siamak.sattar@nist.gov](mailto:siamak.sattar@nist.gov).

<https://doi.org/10.1016/j.engstruct.2018.07.080>

Received 29 August 2017; Received in revised form 18 July 2018; Accepted 25 July 2018

0141-0296/ Published by Elsevier Ltd.

procedures available in the Tier 3 evaluation procedure of ASCE 41: Linear Static Procedure (LSP), Linear Dynamic Procedure (LDP), Nonlinear Static Procedure (NSP), and Nonlinear Dynamic Procedure (NDP). The evaluation results are presented and discussed in detail with a focus on the sources of discrepancy between the two standards as well as between the four evaluation procedures within ASCE 41. Note that, this study was performed before ASCE 41-17 and ASCE 7-16 were published, and represent the seismic assessment of buildings designed per ASCE 7-10, and evaluated per ASCE 41-13. The next section discusses the expected structural performance between the two standards.

## 2. Expected structural performance in ASCE 41 and ASCE 7

The target performance of a building designed in accordance with ASCE 7 depends on the risk category of the building. For a risk category II building, ASCE 7 design provisions are expected to provide less than or equal to 10% probability of collapse at the  $MCE_R$  (risk-targeted maximum considered earthquake). In regards to PBSO, this objective is interpreted as satisfying the Collapse Prevention (CP) performance level at the  $MCE_R$ , which in turn is expected to provide life safety at the design earthquake level ( $2/3 \times MCE_R$ ). ASCE 7 considers *collapse* as the partial or total collapse, and life safety as protection from life threatening damage.

The ASCE 41 evaluation procedure requires collapse prevention at  $BSE-2N = MCE_R$  hazard level and the life safety at  $BSE-1N = (2/3 \times MCE_R)$ , for the Basic Performance Objective of New Buildings (BPON). ASCE 41 defines collapse prevention as the damage state in which the building has a little residual strength and stiffness in the lateral directions, but continues to support gravity loads. In other words, the building is on the verge of partial or total collapse. The Life Safety (LS) performance level in ASCE 41 is defined as the damage state in which structural components have some residual strength and stiffness in all stories and the building carries gravity loads.

Comparing the performances objectives between ASCE 7 and ASCE 41, for a new code-compliant building, shows that both standards intend to produce designs with the same performance levels, *i.e.*, CP at  $MCE_R$  and Life Safety at  $2/3 \times MCE_R$ . However, to the Authors' knowledge, the linkage between the two standards have not been systematically verified for concrete moment frames. Moreover, these two standards use different approaches to achieve their respective performance objectives. The definition of CP and LS are not explicitly aligned between these two standards. The only explicit objective stated in ASCE 7 is a 10% probability of collapse at  $MCE_R$ , which provides 90% confidence of preventing collapse. In addition, the definition of partial or total collapse is not clearly defined in ASCE 7. In ASCE 41, collapse is triggered using a component-based, not system-based approach, wherein each individual component that does not satisfy the acceptance criteria needs to be retrofitted. The component-based definition of collapse in ASCE 41 does not align with the total collapse approach defined in ASCE 7, and does not necessarily align with the partial collapse concept introduced in ASCE 7.

Assuming both ASCE 7 and ASCE 41 standards intend the same definitions for the CP and LS performance levels, this study investigates the relationship between the anticipated performance of a building based on ASCE 41 and ASCE 7 at  $MCE_R$  and  $2/3 \times MCE_R$  hazard levels. The BPON in ASCE 41 is selected in this study for the seismic assessment as the equivalent performance objective for new buildings. Due to the importance of the collapse prevention performance level, the discussion of this paper focuses more on the CP than the LS performance level.

## 3. Design of the archetype buildings

The 4- and 8-story archetype buildings used for this study are presented here as representative of reinforced concrete SMFs built in high seismic regions. The building plan view is shown in Fig. 1. The first

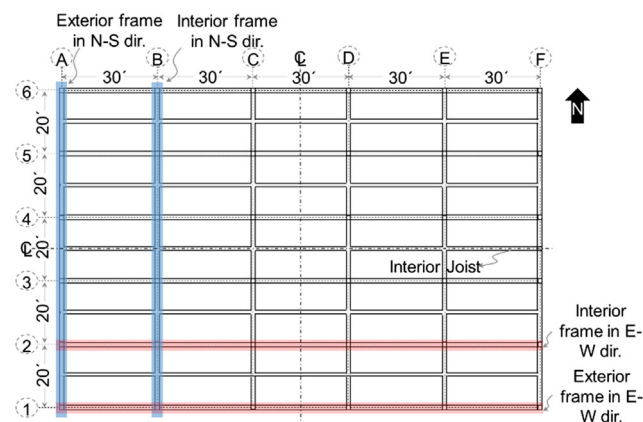


Fig. 1. (a) Plan view of the archetype building (1 ft = 0.3 m).

floor of the buildings has an 18 ft. (5.5 m) story height and the upper floors have a 14 ft. (4.3 m) story height. The archetype buildings are designed in accordance with ASCE 7 and ACI 318-11 [12] using the (1) Equivalent Lateral Force (ELF) procedure and (2) Modal Response Spectrum Analysis (RSA) procedure, to provide a common range of design strength and also to compare the performance of the two designed buildings. The design recommendations from [13] are followed in this study to ensure the practicality of the final design. The difference between the component sizes and reinforcement detailing of the components of the 4-story frame designed using ELF and RSA are minimal for the considered building, and as a result, only the results for the ELF-designed building are presented in this paper. The ELF- and RSA-designed 8-story frame buildings exhibit larger differences. The buildings are considered as Risk Category II, and located in a site with stiff soil (site class D) with spectral response acceleration parameters  $S_S$  and  $S_1$  of 1.5 g and 0.6 g, respectively. The concrete is normal weight ( $150 \text{ pcf} = 23.56 \text{ KN/m}^3$ ) and has a compressive strength of  $f'_c = 5 \text{ ksi} (34.5 \text{ MPa})$ . Grade 60 reinforcing steel is assumed. The dead load including a 4.5 in. (11.4 cm) thick floor slab is 56 psf (2.68 MPa); this load is in addition to the dead load due to the weight of the beams and columns. A 250 plf (3648.3 N/m) façade dead load is also applied to the perimeter beams. The floor and roof superimposed loads are 15 psf (0.72 MPa) and 10 psf (0.48 MPa), respectively. The live load of the floor and roof is 50 psf (2.39 MPa) and 30 psf (1.44 MPa), respectively. The seismic lateral force resisting system consists of special moment frames in both directions with the response modification factor (R) of 8. The building is analyzed and designed for all load combinations in accordance with sections 2.3 and 12.4.2.3 of ASCE 7. Extra load combinations are employed for the components carrying lateral force in two perpendicular directions, in accordance with the recommendations in ASCE 7. The ACI 318 capacity design provisions are also considered in the final design of the columns. Wind loads are also considered in the design. The compliance of the maximum interstory drift ratios with the allowable drift limits prescribed in ASCE 7 is verified in the design. Accidental eccentricity is considered in the design per ASCE 7 recommendations. Appendix A summarizes the typical section sizes and reinforcement of columns and beams in the 4- and 8-story buildings.

## 4. Analysis and assessment of the archetype buildings in ASCE 41

The basic premise of the various evaluation procedures in ASCE 41 is to compare the demand with respect to the capacity, where demand and capacity can be measured in terms of force or deformation. If the capacity of a given component is less than the calculated demand, the component does not pass the acceptance criteria in ASCE 41 and requires retrofit. All components of the archetype buildings including beams, columns, and joints are assessed using two linear and two nonlinear evaluation procedures, defined in ASCE 41. In this study, the

$DCR_N$  is defined as the normalized demand-to-capacity ratio, such that  $DCR_N$  greater than 1.0 identifies the need of retrofit for the component. Employing  $DCR_N$  allows comparison between linear and nonlinear evaluation procedures. The calculation of  $DCR_N$  is different between linear and nonlinear procedures and explained in later sections. The performance of nonstructural components is not considered in this study.

#### 4.1. Building modeling

The first step in assessing the performance of a building is to develop a model that generally simulates the building behavior. Linear elastic and nonlinear models are developed in order to assess the demand in the building components.

##### 4.1.1. Linear simulation models

Three-dimensional (3D) mathematical models are developed in ETABS [14] to quantify the force and deformation demands on the building. All components in the archetype buildings are considered as “primary” components. The gravity and earthquake forces are applied per recommendations in ASCE 41. Concurrent seismic effects in perpendicular directions are considered in the evaluation procedure. Diaphragms are modeled as semi-rigid in the in-plane direction. The base of the columns are modeled as rigid with no translational or rotational degrees of freedom. Geometric nonlinearities (Global  $P-\Delta$ ) effects are considered in the analyses. A 5% modal damping value is used for the models used in the LDP. A sufficient number of modes is included to capture at least 90% of the mass participation in each of the two principal directions. ASCE 41 does not provide clear guidance on whether nominal or expected concrete compressive strength ( $f'_c$ ) shall be used in the stiffness computation of the linear models. Other studies (e.g. [15]) used nominal  $f'_c$  in the stiffness calculation. This study employs the expected  $f'_c$  in computing the stiffness of linear models to follow the common practice. Implementing the expected  $f'_c$  leads to a slightly stiffer model and slightly higher force demands in the components of the linear models.

##### 4.1.2. Nonlinear simulation models

To perform nonlinear procedures, a 3D model is developed in PERFORM 3D (P3D) software [16] to represent each archetype building. Beams and columns are modeled using the concentrated plasticity approach, where each component is modeled with one elastic element in series with two rotational plastic hinges at the member ends, as shown in Fig. 2a. Since the ratio of column flexural-to-shear-strength ( $V_p/V_n$ ) is less than 0.6, the columns are simulated with the purely flexural element [17]. The plastic hinge backbones are modeled with the multilinear moment-rotation type model in P3D, as shown in Fig. 2b. The aggregated response of the elastic element component with two hinges simulates the full backbone response of beams or columns including elastic stiffness,  $K_e$ , hardening,  $K_s$ , yield strength,  $M_y$ , ultimate strength,  $M_c$ , post peak strength degradation,  $K_c$ , and residual

strength,  $C$ . A similar modeling approach for concrete frames has been used in previous studies [17,18]. All modeling parameters except the elastic stiffness,  $K_e$ , are assigned to the rotational springs in Fig. 2a. The “a” and “b” parameters, shown in Fig. 2b, are computed per Tables 10-7, 10-8, and 10-10 of ASCE 41, as a function of material properties, detailing, and loading characteristics of the components of interest. The beam/column flexural strength,  $M_c$ , is computed based on principle of mechanics [12], and  $M_c/M_y$  is considered as 1.2. ASCE 41 does not provide any specific recommendation on the calculation of post peak degradation and residual strength. However,  $K_c$  is limited by the “b” value. 20% residual strength is considered for the flexural strength of the members. In order to prevent convergence errors, the residual strength of the member does not drop to zero in the numerical model. The effective stiffness of the elastic element is calculated based on the recommendations of ASCE 41, between 30% and 70% of flexural rigidity, depending on the level of the axial load in the component [4]. The plastic hinge model employed in this study is considered as a validated model, as the modeling parameters are developed based on the numerous experimental and analytical studies. The backbone curves in ASCE 41 are the envelope for the hysteretic behavior [19]. In the absence of recommendations in ASCE 41 for cyclic degradation of the components, the degradation parameters for beams and columns are calibrated with respect to a typical reinforced concrete beam-column with seismic detailing. Fig. 3 shows the calibration of the cyclic response of the plastic hinge for a beam tested by Matamoros [20]. Fig. 3 also serves as a verification for the modeling approach adopted in this study. Please note that Fig. 3 does not try to calibrate the strength and stiffness of the response, and those modeling parameters are computed using the modeling approach explained above. In this study, due to software limitations, the cyclic degradation of the column response is considered after the peak response is reached in the nonlinear models. Geometric nonlinearities ( $P-\Delta$ ) are considered in the analyses. Beam-to-column connections are modeled with panel zone elements only in the N-S direction frames due to software limitations in modeling the panel zones in two perpendicular directions. The N-S frames have a higher shear demand at the joints and therefore, the N-S frame is selected for modeling the beam-to-column joints. The panel zone element captures the key characteristics of the joint including yield, ultimate strength, and post peak strength loss. This study does not consider the uncertainty embedded in the modeling approach or material properties.

#### 4.2. Linear static procedure: computation

The analysis procedure in LSP is similar to the ELF design procedure in ASCE 7, where an inverted triangular static load is applied to an elastic model and force and deformation demands are computed and compared with the capacity. In ASCE 41, the component actions are divided into force- and deformation-controlled actions. Force-controlled actions experience a significant strength loss with no or limited inelastic deformation; however, deformation-controlled actions undergo a larger inelastic deformation before strength loss occurs. For

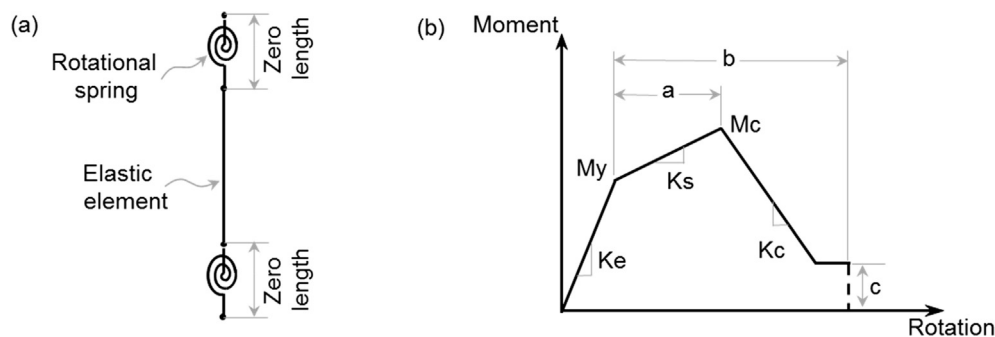


Fig. 2. Illustration of (a) column/beam flexural models implemented in P3D and (b) the column/beam flexural response.

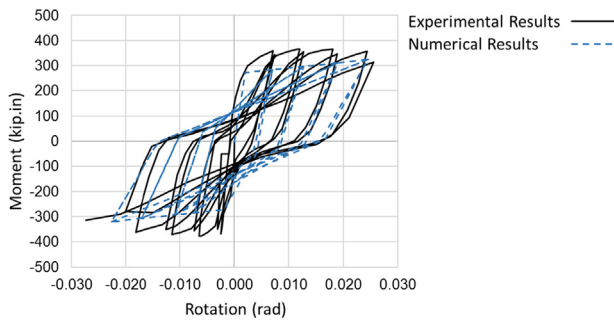


Fig. 3. Calibration of the cyclic response of the numerical model for a reinforced concrete beam (C5-00) tested by Matamoros [20] (1 kip = 4.448 kN, 1 in = 0.025 m).

computing the  $DCR_N$  under the force-controlled actions, the component demand,  $Q_{UF}$ , is divided directly by the lower-bound component capacity,  $Q_{CL}$ , as shown in Eq. (1). However, in deformation-controlled actions, the capacity is multiplied by an  $m$ -factor in order to establish a direct comparison between the demand,  $Q_{UD}$ , and expected capacity,  $Q_{CE}$ , as shown in Eq. (1). The  $m$ -factor accounts for the ductility experiences by the component in a specific action.

$$DCR_N = \begin{cases} \frac{Q_{UF}}{\kappa Q_{CL}} & \text{force-controlled} \\ \frac{Q_{UD}}{m \kappa Q_{CE}} & \text{deformation-controlled} \end{cases} \quad (1)$$

$$(a) \quad Q_{UF} = Q_G + \frac{Q_E}{C_1 C_2 J}, \quad (b) \quad Q_{UD} = Q_G + Q_E \quad (2)$$

In Eq. (1),  $\kappa$  is the knowledge factor, and assumed to be equal to 1.0. ASCE 41 states that  $Q_{UF}$  can be computed using either directly from Eq. (2-a) or limit-state analysis. The former is more common in practice and is adopted in this study.

In Eq. (2),  $Q_E$  is the action caused by computed earthquake forces based on the selected hazard level, and  $Q_G$  is the action caused by gravity forces.  $J$  is the force delivery reduction factor, which is computed as the minimum of the demand-to-capacity ratios of components delivering force into the component of interest, but not less than 2.0.  $C_1$  and  $C_2$  are amplifiers that account for the inelastic response of the component [4].  $Q_{UD}$  is computed based on Eq. (2-b). In Eqs. (1) and (2),  $Q$  represents the general capacity or demand and can be replaced by flexural ( $M$ ), axial ( $P$ ), or shear ( $V$ ). For computation of the  $DCR_N$  of the columns, the interaction between the moments and axial force, i.e.,  $P$ - $M_2$ - $M_3$ , is considered.

#### 4.3. Linear static procedure: results

All components in the archetype buildings are evaluated using the LSP at the CP and LS performance levels. Figs. 4a, c, and 5a show the  $DCR_N$  for various actions of the components in the E-W direction for the interior frame. In these figures, the  $DCR_N$  values greater than 1.0 are underlined, illustrating that the components do not pass the ASCE 41 acceptance criteria. Due to the symmetry of the frames, the results are reported for half of the frame in Figs. 4 and 5. Fig. 4a shows that the flexural-axial response of all columns in the first story as well as the exterior column in the second story of the 4-story building fail to satisfy the acceptance criteria of ASCE 41 at the CP performance level, while the response of the remainder or the components pass. The  $DCR_N$  values are computed for the components of the E-W exterior frame as well as the N-S exterior and interior frames. All components of the 4-story building pass the ASCE 41 acceptance criteria at the LS performance level. LSP assessment results for the 8-story ELF-designed building at the CP performance level show that more components, including beams and columns, in comparison with the 4-story building, fail the acceptance criteria given in ASCE 41. The unsatisfactory components are

distributed over the height of the building. The results also show a general increase in the  $DCR_N$  values as the building height increases. At the LS performance level, only columns in the first story of the ELF-designed building fail the acceptance criteria, where the maximum  $DCR_N$  is 1.82. Comparison between the results of the 8-story RSA- and ELF-designed building (Figs. 4c and 5a) reveals that more columns in the RSA-designed building do not pass ASCE 41 acceptance criteria, while most components have a higher  $DCR_N$  ratio compared to the ELF-design building. This observation indicates a better performance of the ELF-designed building per ASCE 41 evaluation procedure. The lower  $DCR_N$  values in the columns of the ELF-designed buildings occur due to the higher strength of the columns in that building. The  $DCR_N$  of the beams for positive bending in the RSA-designed building are slightly lower than the  $DCR_N$  values in the ELF-designed building in lower stories due to a slight higher strength of the beams of the RSA-designed building in those stories. A similar trend is observed between the results of 8-story RSA- and ELF-designed building at the LS performance level. Analysis results show that beam-to-column joints pass the acceptance criteria in ASCE 41 when LSP is employed with a large margin of safety. Analysis results show that none of the buildings pass the ASCE 41 target performance at the CP performance level for all of the components when LSP is employed in the assessment.

#### 4.4. Linear dynamic procedure: computation

The computation of  $DCR_N$  values in the LDP is the same as the LSP, except for that the component demands are computed from response spectrum analysis of the linear elastic models developed for the LSP. The effective seismic weight is computed as dead loads plus 20% of the unreduced design floor live loads. The responses of different modes are combined using the square-root-of-sum-of-squares (SRSS) to obtain the maximum deformation and force values. The provisions for LDP are similar to those for the RSA procedure in ASCE 7, except that ASCE 41 does not require scaling the base shear to 85% of the base shear from ELF procedure.

#### 4.5. Linear dynamic procedure: results

Figs. 4b, d, and 5b show the LDP results for an interior frame in the E-W direction of the ELF- and RSA-designed frames, respectively. The assessment results show that all components in the 4-story building pass the ASCE 41 acceptance criteria at the CP and LS performance levels. However, some of the components in the 8-story RSA- and ELF-designed buildings do not satisfy the ASCE 41 expected performance.

Similar to the LSP procedure, more components fail the acceptance criteria in the RSA-design than ELF-designed building with higher  $DCR_N$  values, when LDP is employed for both CP and LS performance levels. However, the assessment results show that, in general, more components pass the ASCE 41 acceptance criteria when LDP is employed rather than LSP. Moreover, in general, LDP produces lower  $DCR_N$  values than LSP mainly due to the lower force demand computed for various actions in the LDP.

#### 4.6. Nonlinear static procedure: computation

The nonlinear models are subjected to a monotonically increasing displacement load pattern proportional to the fundamental mode shape of the structure in the direction under consideration until the displacement in the control node of the building (center of the mass at the roof) exceeds the target displacement,  $\delta_t$ . The target displacement represents the expected displacement likely to be experienced by the structure at a specific seismic hazard level. Table 1 summarizes the calculations of the target displacement for the 4- and 8-story buildings in the E-W direction. The archetype buildings have different periods in the E-W and N-S directions, and two separate pushover analyses are conducted for each direction.

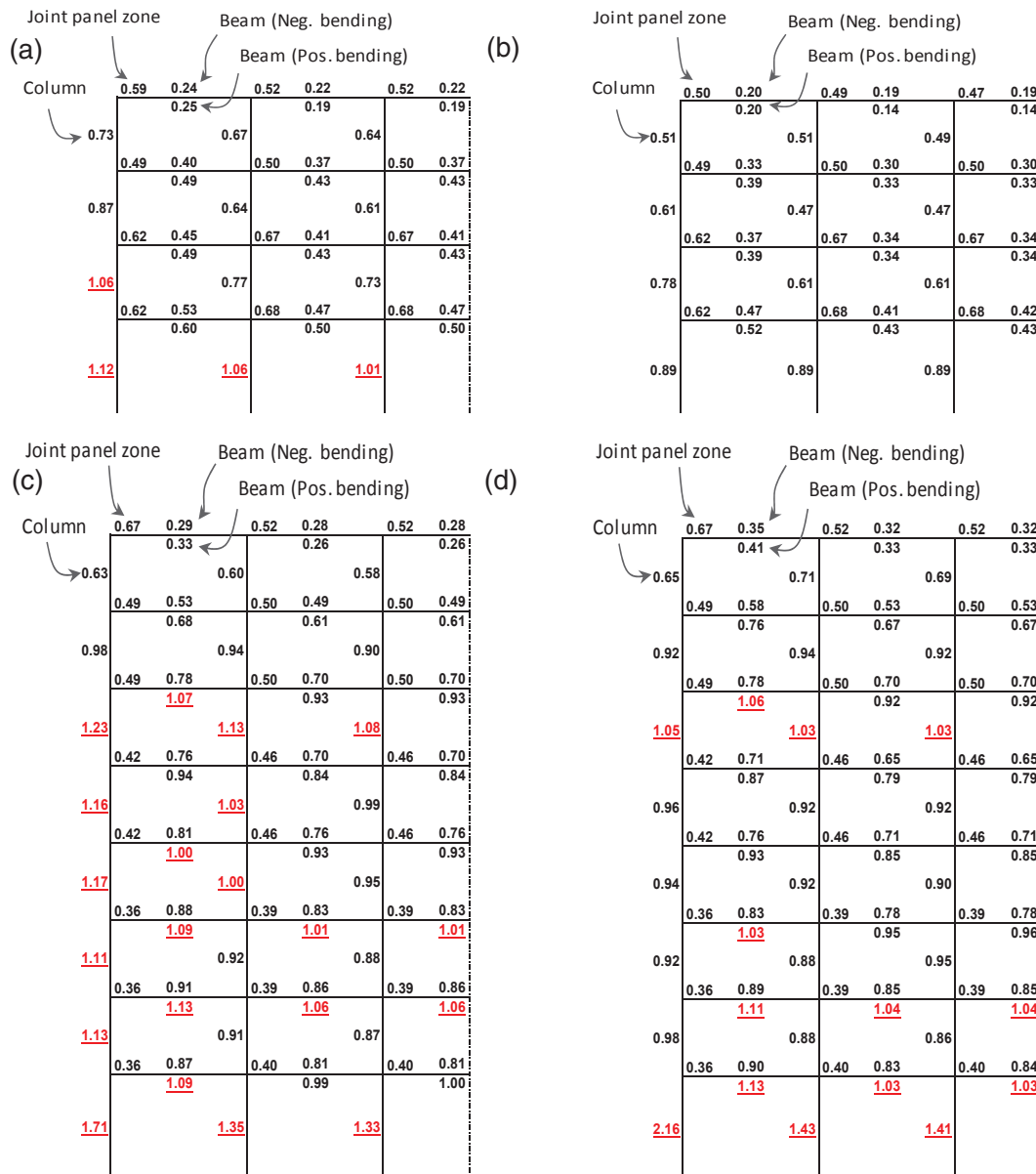


Fig. 4. Normalized demand-to-capacity ratio ( $DCR_N$ ) values for beams and columns in the interior E-W direction frame and beam-to-columns joints in the N-S direction frame at the Collapse Prevention performance level for: (a) 4-story ELF-designed building using LSP; (b) 4-story ELF-designed building using LDP; (c) 8-story ELF-designed building using LSP; (d) 8-story ELF-designed building using LDP. [Due to symmetry, the results are presented for half of the frame].

The  $DCR_N$  is computed for each component in the nonlinear static procedure by dividing the plastic deformation demand by the permissible deformation, i.e., acceptance criteria, for a given performance level. The deformation demands of the components in the nonlinear models are measured at the target displacement. The acceptance criteria for each component are computed based on Tables 10-7, 10-8, and 10-10 of ASCE 41 as a function of parameters such as transverse reinforcement ratio, axial and shear force, compressive strength of concrete, and reinforcement detailing.

#### 4.7. Nonlinear static procedure: results

Fig. 6 shows the pushover response of an interior frame in the E-W direction of the 4- and 8-story buildings. The drift levels at which each building reaches the various performance levels are highlighted in this figure, with the exception of the column response for the 8-story RSA-designed building for which the analysis failed to converge before the column limits were reached. At the target displacement corresponding

to the collapse prevention performance level, beams in the second floor of the 4-story building and beams in the second and third floors of the 8-story RSA-designed building fail to meet the ASCE 41 acceptance criteria exhibiting  $DCR_N$  greater than 1.0 as shown in Fig. 7. The rest of the components in these buildings as well as all components in the 8-story ELF-designed building have  $DCR_N$  ratio significantly less than 1.0 (i.e.,  $DCR_N < 0.7$ ). At the LS target displacement, all the components of the archetype buildings pass the ASCE 41 acceptance criteria. The response of the frames in the N-S direction is different from the response of frames in the E-W direction. All the components of the three archetype buildings pass the acceptance criteria at both LS and CP performance levels, when the frame is pushed in the N-S direction. The better performance of the buildings in the N-S direction is due to having stronger beams in this direction.

#### 4.8. Nonlinear dynamic procedure: computation

In order to assess the performance of the buildings using the NDP,

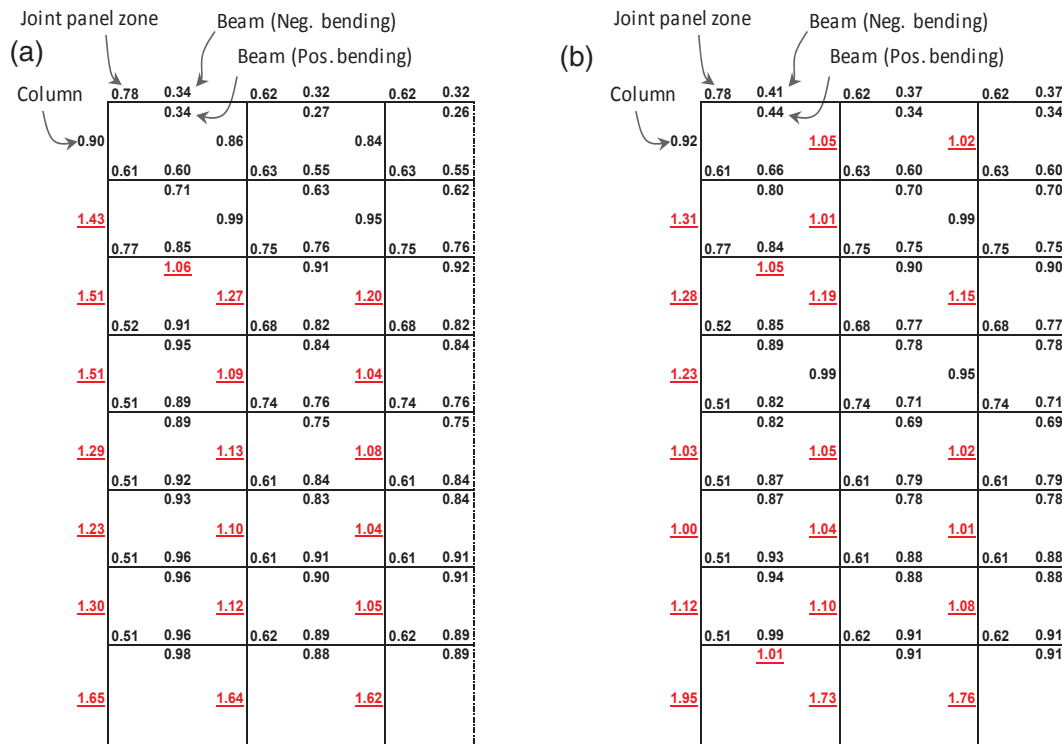


Fig. 5. Normalized demand-to-capacity ratio ( $DCR_N$ ) values for beams and columns in the interior E-W direction frame and beam-to-column joints in the N-S direction frame at the Collapse Prevention performance level for: (a) 8-story RSA-designed building using LSP, (b) 8-story RSA -designed building using LDP.

the nonlinear models are analyzed dynamically for 14 pairs of ground motions, selected from the 22 pairs in FEMA P-695 [21]. The ground motion selection procedure is similar to the approach used by Speicher and Harris [10]. The ground motions are selected to minimize the difference between the scaled square-root-of-sum-of-squares of two horizontal components of each pair and the  $MCE_R$  target spectrum between  $0.2 \times T_1$  and  $2 \times T_1$ , where  $T_1$  is selected as the minimum or maximum of the first fundamental periods in the two perpendicular directions of the building for the lower and upper bound periods, respectively. The selected ground motions are further scaled to ensure that no points in the average of the spectrum produced from selected records are less than the target spectrum in the period range of interest. Fig. 8 shows the individual and average selected scaled ground motions for the three archetype buildings overlaid on the  $MCE_R$  spectrum. The scale factors of the ground motions selected for the CP performance level assessment is multiplied by 2/3 to be used in the LS performance level evaluation. Buildings frames are modeled with 3% modal damping. In addition to the modal damping, a 0.3% Rayleigh damping (elastic stiffness component only) is added to the model, per recommendations by CSI [16]. Global P- $\Delta$  effects are included in the analysis. In each response history analysis, two perpendicular components of each ground motion are scaled using the same scale factor, and applied simultaneously to the building along the E-W and N-S directions.

The maximum deformation demand of each component is computed

Table 1  
Parameters computed to determine the target displacement,  $\delta_t^*$ .

Building	Direction	$T_e^{**}$ (s)	$C_{0(BSE1)}$	$C_{0(BSE2)}$	$C_1$	$C_2$	$S_{a(BSE1)}$ (g)	$S_{a(BSE2)}$ (g)	$\delta_t$ (BSE1) (in/in)	$\delta_t$ (BSE2) (in/in)
4-story	E-W	1.62	1.23	1.22	1	1	0.34	0.51	0.0176	0.024
8-story (ELF)	E-W	2.34	1.31	1.28	1	1	0.26	0	0.013	0.019
8-story (RSA)	E-W	2.91	1.30	3.06	1	1	0.20	0.29	0.015	0.023

\* The definition of parameters are presented in Section 7.4.3.3 of ASCE 41.

\*\*  $T$  is computed using Eigenvalue analysis in PERFORM 3D.

for each time history analysis, and divided by the permissible capacity from ASCE 41 to compute the  $DCR_N$ . ASCE 41 allows using the average response when more than 10 pairs of records have been used in the NDP. As a result, the  $DCR_N$  from 14 time history analyses are averaged to represent the mean response.

#### 4.9. Nonlinear dynamic procedure: results

Figs. 9 and 10 summarize the  $DCR_N$  results and include the statistical mean, median, and mean plus one standard deviation for the selected beams and columns, respectively. Figs. 9 and 10 show that the average ratios of the plastic rotation demand to the acceptance criteria is considerably lower than 1.0, meaning that these components satisfy the CP performance level in ASCE 41. Similar results developed for the other columns, beams, and beam-to-column joints in the archetype buildings show that all components meet the acceptance criteria in ASCE 41 for both CP and LS performance levels when NDP is employed for the assessment. These results suggest that the NDP is less conservative than the linear procedures.

### 5. Discussion of the assessment results

The analysis results show that the performance of RC moment frame buildings designed per requirements in ASCE 7 does not necessarily satisfy the performance required by ASCE 41. Moreover, the results

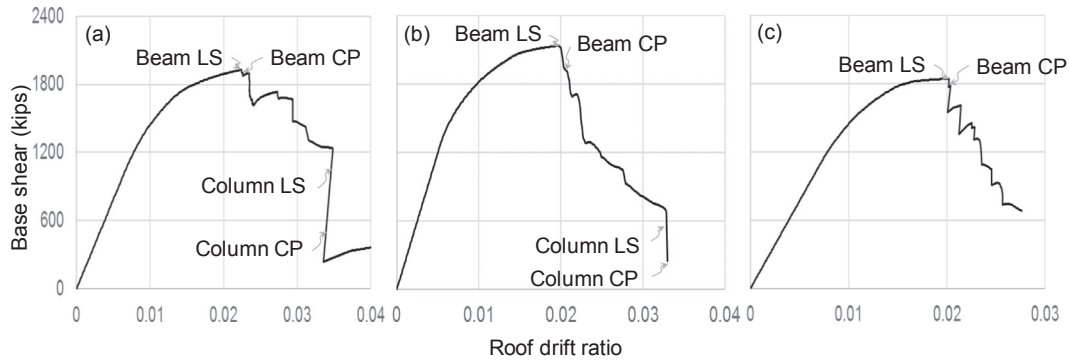


Fig. 6. Pushover analysis results in the E-W direction of the (a) 4-story; (b) 8-story ELF-designed; (c) 8-story RSA-designed frames (1 kip = 4.448 kN).

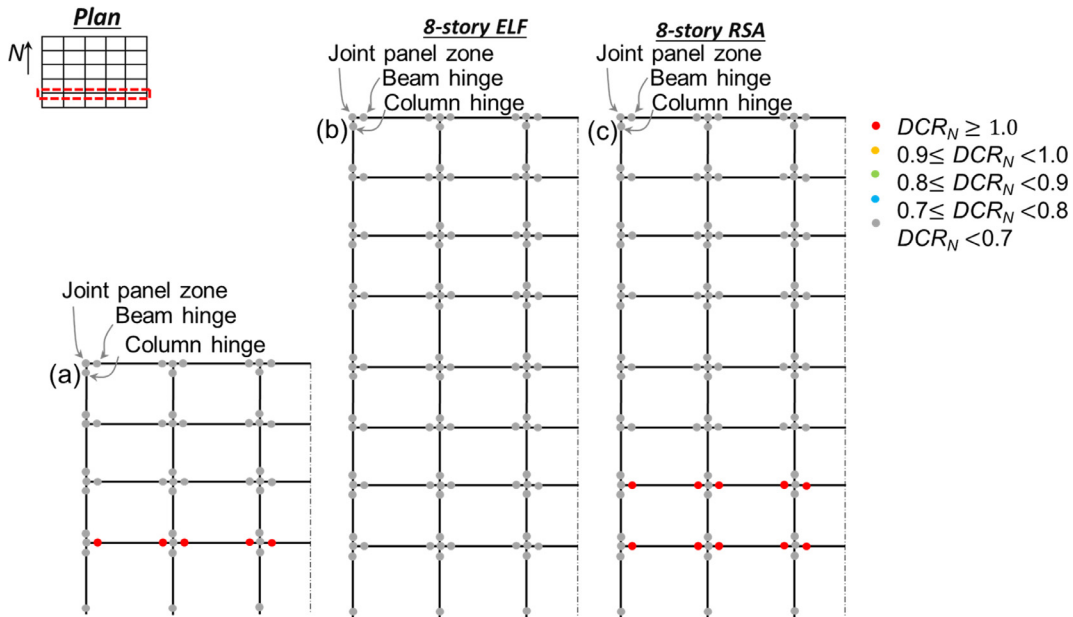


Fig. 7. Pushover analysis results for an interior frame in the E-W direction of the (a) 4-story; (b) 8-story ELF-designed; (b) 8-story RSA-designed frames.

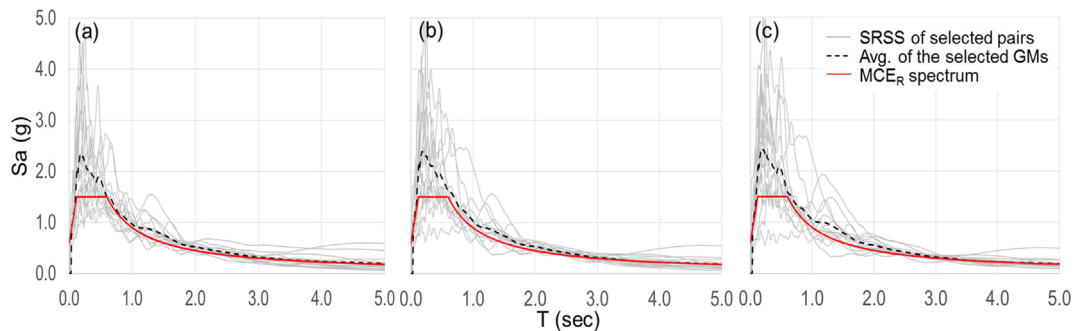


Fig. 8. Response spectra of selected scaled ground motions compared with the target spectrum for: (a) 4-story; (b) 8-story ELF-designed; (c) 8-story RSA-designed buildings.

show that the four evaluation methodologies in ASCE 41 may lead to different retrofitting decisions depending on the evaluation method used. In other words, a building component may pass the acceptance criteria for one procedure while requiring retrofitting when another procedure is employed. This section discusses the details of the differences between ASCE 41 and ASCE 7 and differences among the four evaluation procedures in ASCE 41; these details shed light on potential ways to remove some of the discrepancies between ASCE 41 and ASCE 7 and to align the four evaluation methodologies in ASCE 41.

### 5.1. Linear static procedures

The prescriptive design process, similar to the linear procedure, is based on analyzing a linear elastic model. The distribution of the forces along the height of the elastic model is the same between the ELF-designed building and linear static evaluation procedure, and also between the RSA-designed building and linear dynamic evaluation procedure. Despite these similarities, the analysis results show significant inconsistencies between the expected performance in ASCE 7 and results of the linear evaluation procedures in ASCE 41. These differences

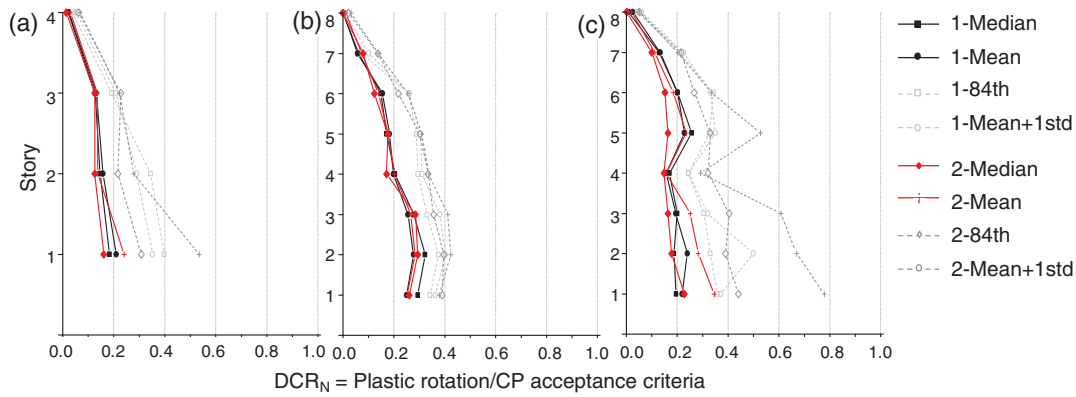


Fig. 9. Statistical information of the beam response assessed using NDP at the CP performance level for the (a) 4- story; (b) 8-story ELF-designed; (c) 8-story RSA-designed buildings. The results are presented for beams in the bay B-C of the E-W interior frame. [1- and 2-, in the legend, represent two ends of each beam.]

arise from various sources in the computation of demand and capacity as well as differences in the analysis procedures.

The effective stiffness considered for beams and columns in the design and assessment methodologies do not match. Table 2 compares the cracked stiffness modifier in ACI 318 and ASCE 41. ACI 318 defines the stiffness modifier as a range with no specific guidance on the exact value. However, the stiffness modifier in ASCE 41 varies with respect to the axial load ratio. Different stiffnesses employed in design and assessment induce different force and displacement demands in the linear models that in turn leads to different demand-to-capacity ratios.

Moreover, the gravity load of the components considered in the design and evaluation procedures are not the same. The ASCE 7 load cases require  $(1.2 + 0.2S_{DC})D$ ,  $1.2D$ ,  $0.9D$ , and  $(0.9 - 0.2S_{DC})D$ , while ASCE 41 considers  $1.1D$  and  $0.9D$ , where  $D$  is dead load on the structure. In addition to the component gravity loads, the  $P - \Delta$  load combination is defined here as  $1.2D + 0.25L$  and  $1.0D + 0.25L$  for design (ASCE 7) and assessment (ASCE 41) procedures, respectively. The higher gravity load in the design procedure induces higher compression and bending moment demands in the building components.

The capacity of the structural components is not computed in the same manner between the design, i.e., ASCE 7, and assessment, i.e., ASCE 41, procedures. The nominal or probable strength of the components is used in the design procedure, where the nominal strength is computed using the nominal material properties, and the probable strength is computed using the yield strength of the steel reinforcement multiplied by 1.25. In the evaluation procedure, the capacity of the component is computed based on expected or nominal material properties depending on type of the action, i.e., deformation- or force-controlled. The expected capacity of the components is computed using

Table 2

Cracked stiffness modifier for concrete components in ACI 318 and ASCE 41.

ACI 318		ASCE 41	
Beam	0.35–0.5	$P \geq 0.5A_g f'_c$	0.7
Column	0.5–0.7	$P \leq 0.1A_g f'_c$	0.3

\*  $P$  is the axial load in the component;  $A_g$  is the gross cross sectional area;  $f'_c$  is the compressive strength of concrete.

$1.25f_y$  and  $1.5f'_c$ , which differs from the values used in prescriptive design. Although the component capacity in design and assessment is multiplied by a resistance factor  $\phi < 1$  and  $\phi = 1$ , respectively, the underlying equations to compute component capacity are the same for most of the actions in design and assessment.

Similar to the differences in the computations of demand and capacity, the analysis procedures between ASCE 7 and ASCE 41 do not align. ASCE 7 caps the period considered in the analysis to  $C_u T_u$ , where  $C_u$  is a coefficient for upper limit period and  $T_u$  is the approximate fundamental period. However, ASCE 41 allows for the period to be computed using eigenvalue analysis (analysis period). For buildings with an analysis period greater than  $C_u T_u$ , the demands computed per ASCE 7 would be higher than those demands computed using ASCE 41, because the lower period is associated with a higher spectral acceleration on the response spectrum. Moreover, in the ASCE 7, procedure the structural demand computed from analysis is divided by a system-specific seismic design modification coefficient, i.e., the  $R$ -factor, to account for ductility of the building. In contrast to ASCE 7, ASCE 41 distinguishes the demand computation in the force- and deformation-controlled actions. For deformation-controlled actions, the ASCE 41

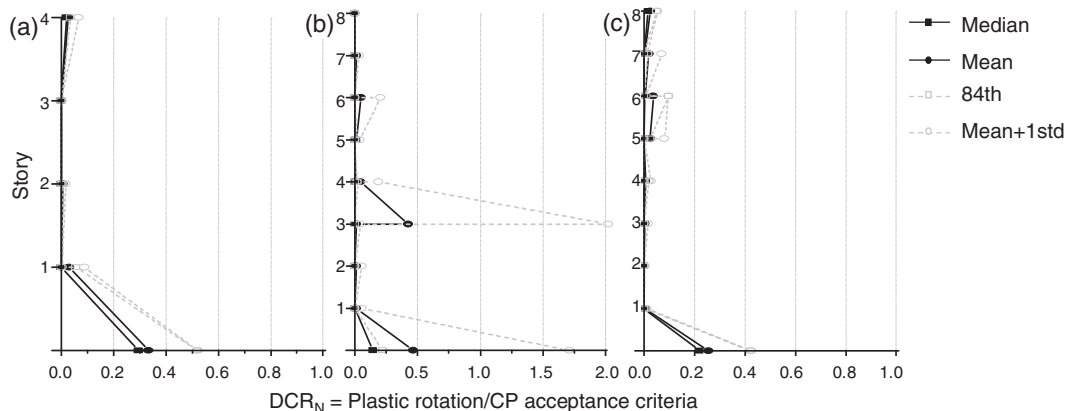


Fig. 10. Statistical information of the column response assessed using NDP at the CP performance level for the (a) 4- story; (b) 8-story ELF-designed; (c) 8-story RSA-designed buildings. The results are presented for columns at the intersection of intersection of grid lines 2 and C.

**Table 3**

Demand ( $M_{UD}$ ) and capacity ( $M_{CE}$ ) of a beam in the 2<sup>nd</sup> floor, between grids A and B on grid 2, of the 8-story ELF-designed building. [The ASCE 41 results are presented for the linear static procedure. “+” and “-” indicate the results for positive and negative moments]. [1 ksi = 6.89 MPa, 1 kip = 4.45 kN, 1 kip.ft = 1.356 kN m].

Response	$f_c$ (ksi)	$f_y$ (kip)	$C_1$	$C_2$	$J$	$M_{UD}^+$ (kip.ft)	$M_{UD}^-$ (kip.ft)	$M_{CE}^+$ (kip.ft)	$M_{CE}^-$ (kip.ft)	$\phi$	$R$	$m^+$	$m^-$	$DCR^+$	$DCR^-$
ASCE 41 @ BSE-2N	7.5	75	1	1	2	1620	1740	233	383	1.0	1	7	5.6	0.99	0.81
ASCE 41 @ BSE-1N	7.5	75	1	1	2	1063	1184	233	383	1.0	1	6	4.6	0.76	0.67
ASCE 7	5.0	60	-	-	-	1168	1912	183	303	0.9	8	-	-	0.89	0.88

procedure divides the demand by a component specific  $m$ -factor. The idea behind the  $m$ - and  $R$ -factors is the same, i.e., considering ductility of the element or building system. However, the values of the  $m$ - and  $R$ -factors are not the same. ASCE 7 specifies a higher  $R$ -factor compared to the ASCE 41  $m$ -factor for reinforced concrete moment frames which implies a lower component demand in design compared to the assessment. For force-controlled actions, the demand is computed by dividing the earthquake portion of the total demand by a force-delivery  $J$  factor.  $J$  is defined as the smallest demand to capacity ratio of the components in the load path delivering force to the component of interest or alternatively, as 2.0 for a high level of seismicity.  $J$  is intended to compute the maximum force delivered to component of interest by other components. The differences in the value of  $R$  (in ASCE 7) and  $J$  (in ASCE 41) yield different demand in the response of the components with force-controlled actions. Moreover,  $J$  is only applied to the earthquake portion of demand, unlike the  $m$ - or  $R$ - factors.

The aforementioned differences in the computation of demand and capacity in ASCE 41 and ASCE 7 lead to inconsistent demand-to-capacity ratios between the two standards. Tables 3 and 4 summarize demand, capacity, and various parameters employed in the calculation of the demand-to-capacity ratio for a beam and column in the 8-story ELF-designed building. The  $DCR_N$  values for ASCE 41 are reported for the BSE-1N and BSE-2N hazard levels. Since ASCE 7 input ground motion intensity is associated with the life safety performance level, comparing the ASCE 7 demand-to-capacity ratios to the ASCE 41 ratios at BSE-1N can be considered as a “fairer” comparison than BSE-2N. Table 3 shows that the positive and negative demand-to-capacity ratios computed per ASCE 7 for the beam are 17% and 31% higher than ASCE 41 values at BSE-1N, respectively. However, Table 4 shows that the ASCE 7 demand-to-capacity ratio for the selected column is 65% less than ASCE 41 values BSE-1N. Among the various sources of differences mentioned earlier between ASCE 41 and ASCE 7, the difference between the  $R$ - and  $m$ -factors play the most important role in the discrepancy between the demand-to-capacity ratios of two standards. Making  $R$ - and  $m$ -factor values more consistent can remove most of the inconsistency between the two standards in the calculation of components demand-to-capacity ratios for the buildings studied here.

### 5.2. Linear dynamic procedure

The higher shear force computed in the LDP of ASCE 41 in comparison to the RSA procedure in ASCE 7, due to the lack of scaling the base shear in the LDP, leads to higher force demands in the assessment models than RSA-designed models. In addition, the differences mentioned earlier regarding the computation of demand and capacity in the LSP still exist in the LDP. These differences contribute to the

**Table 4**

Demand ( $M_D$ ) and capacity ( $M_C$ ) of a column in the 1<sup>st</sup> story on grid B and 2 of the 8-story ELF-designed building. LSP-LS. [The ASCE 41 results are presented for the linear static procedure. “x” and “y” indicate the results for the principal axes of the column]. [1 ksi = 6.89 MPa, 1 kip = 4.45 kN, 1 kip.ft = 1.356 kN m].

Response	$f_c$ (ksi)	$f_y$ (kip)	$C_1$	$C_2$	$J$	$M_{Dx}$ (kip.ft)	$M_{Dy}$ (kip.ft)	$P$ (kip)	$M_{Cx}$ (kip.ft)	$M_{Cy}$ (kip.ft)	$\phi$	$R$	$m$	$DCR$
ASCE 41 @ BSE-2N	7.5	75	1	1	2	3685	1054	643	931	264	1.0	1	3.0	1.35
ASCE 41 @ BSE-1N	7.5	75	1	1	2	2458	703	652	936	268	1.0	1	2.5	1.07
ASCE 7	5.0	60	-	-	-	1907	494	386	691	179	0.9	8	1.0	0.38

inconsistency between the LDP results of ASCE 41 and ASCE 7 RSA-designed buildings.

Linear dynamic procedure assessment results of the 8-story RSA- and ELF-designed buildings reveal that a select number of exterior columns have  $DCR_N$  values in the range between 3 and 6, which is significantly greater than 1.0, and is not expected for a code-compliant building.

A similar trend is also observed when LSP is employed. Analysis results indicate that the large  $DCR_N$  corresponds to the case where the column is in tension; the flexural strength of a column under tension in the P-M-M interaction diagram is very low. In the ASCE 41 linear procedures, the flexural strength of the column is computed at an axial force level which is computed as a force-controlled action regardless of tension or compression. This method may cause two issues: (1) the assumption of a brittle failure for a column under tension is not realistic, and (2) consideration of tension as a force-controlled action can lead to unrealistically high tensile demand and as a result, an unrealistically low flexural strength of the columns that is not realistic. One possible solution for this problem is to consider the axial tension in the column as a deformation-controlled action, but a question still arises in regard to which  $m$ -factor should be considered for the axial force in the columns.

### 5.3. Nonlinear static procedure

In contrast to the linear procedures where the demand is measured primarily in terms of force in the components, in the nonlinear static procedure the demand in the component is primarily measured in terms of deformation. The capacity of the elements, for a deformation-controlled action, in the linear procedures is computed in terms of strength using principals of mechanics and then multiplied by an  $m$ -factor. However, in the nonlinear procedures, the capacity of the elements at various performance levels is computed as a fraction of the deformation at the peak strength of the element. Because of these fundamental differences in the computation of demand and capacity in the linear and nonlinear static procedures, providing a direct comparison between the results from NSP and the linear or design procedure is not straightforward. The results from the nonlinear static procedure assessment show lower  $DCR_N$  values than those computed using linear procedures for the majority of the components of the frames. Similar to the linear evaluation procedures, the findings also show that the code-compliant buildings do not always meet the performance goal for the ASCE 41 NSP evaluation at the CP performance level. The results show that, in general, more components pass the ASCE 41 acceptance criteria with lower  $DCR_N$  ratios when NSP is employed in comparison with the LSP or LDP. This difference is larger when NSP is compared against the LSP.

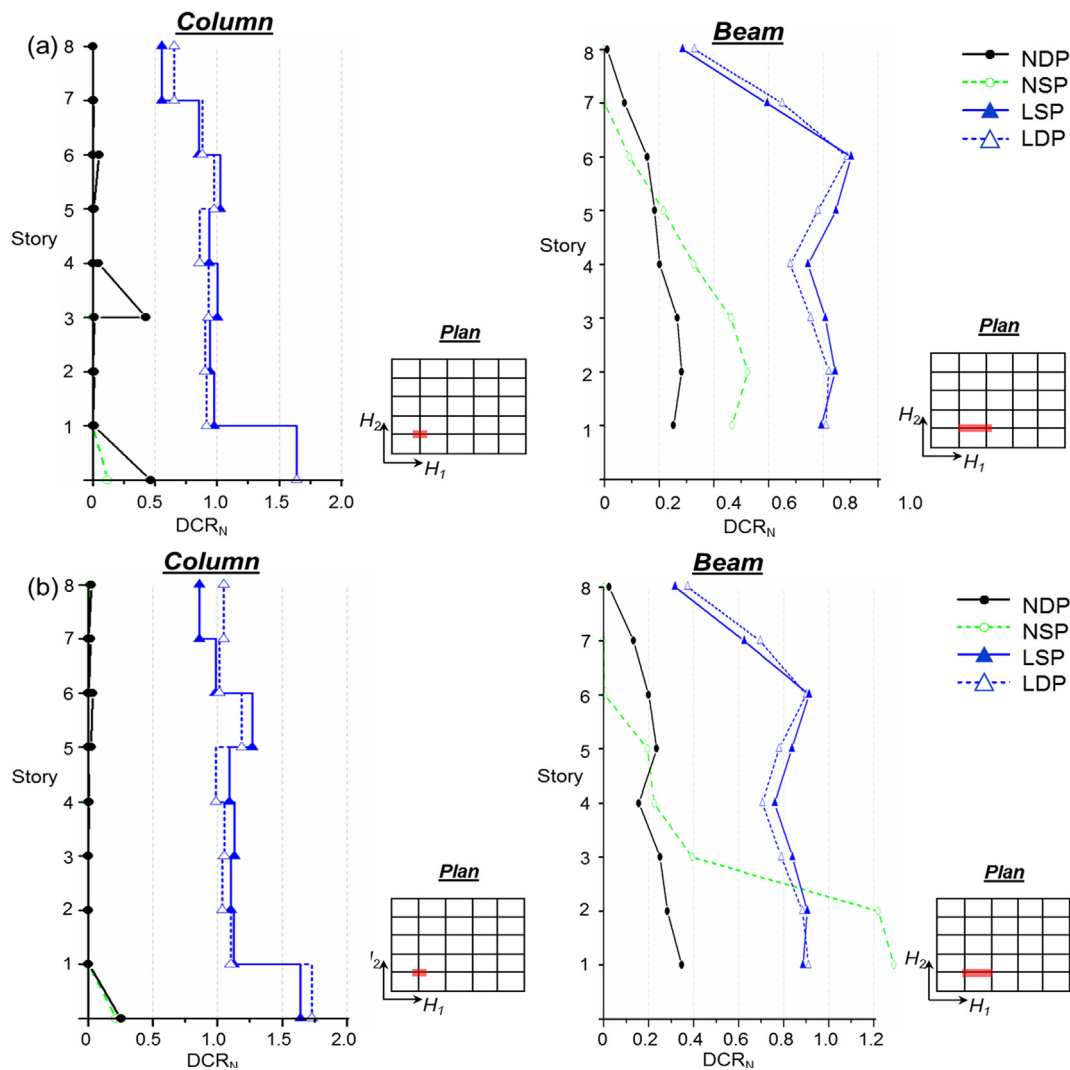


**Fig. 11.** Normalized demand-to-capacity ratio for selected beams and columns in the (a) 8-story ELF-designed and (b) 8-story RSA-designed frames using four evaluation procedures in Tier 3 analysis of ASCE 41. [For nonlinear procedures the average response is presented for columns; for beams the envelope of the response between two hinges at the end are shown.]

The NSP results also show the poor performance of the RSA-designed building.

#### 5.4. Nonlinear dynamic procedure

The analysis results indicate that the NDP is the only procedure for which all components of the ASCE 7 code-compliant archetype buildings pass the ASCE 41 acceptance criteria at the CP and LS performance levels. The better performance of the NDP in comparison to the NSP is likely due to capturing the higher mode effects in a more accurate and less conservative manner. Fig. 11 shows the comparison between the evaluation results for beams and columns using four different evaluation procedures in Tier 3 analysis of ASCE 41. These results show a general inconsistency between the results of the various evaluation procedures, implying that the four evaluation procedures in ASCE 41 are not calibrated with respect to each other. For most of the components, linear procedures are more conservative than nonlinear procedures. This trend is expected to some extent. It is generally believed that when more sophisticated analysis models such as nonlinear models are employed and more effort is devoted to the analysis, the conservatism in the evaluation procedure is expected to be reduced. However, a challenging issue is whether the level of inconsistency between linear and nonlinear assessment procedures is acceptable. For instance, results

in Fig. 11 show that the  $DCR_N$  value predicted by the LSP at the base of the column in the first story of the RSA-designed building is about six times larger than that predicted by NDP. If the NDP is considered as the most accurate evaluation procedure, then one can conclude that the linear procedures are overly conservative. The conservatism in the linear procedure is expected; however, the level of this conservatism is an issue which may need to be revisited by the appropriate standards committee. Increasing the m-factors used in the linear procedures can reduce some of this conservatism.

Moreover, Fig. 11 shows that the NSP can predict the lowest and largest  $DCR_N$  values in comparison to the other evaluation procedures. This result contradicts the perception that linear results are always more conservative than nonlinear results. The acceptance criteria for the components in the nonlinear models used in the NDP are the same as those used in the NSP. So, one could conclude that the difference in  $DCR_N$  values between the NSP and NDP is due to the difference in deformation demand induced in the components, which is caused by the differences in the applied load and analyses of the buildings. For illustration purposes, Fig. 12 shows the moment-rotation response of the plastic hinge located at the left side of the selected beam shown in Fig. 11a for a single earthquake record used in the NDP in comparison with the NSP results. This figure shows that the maximum plastic rotation of the selected hinge computed using the NSP is 1.6 times bigger

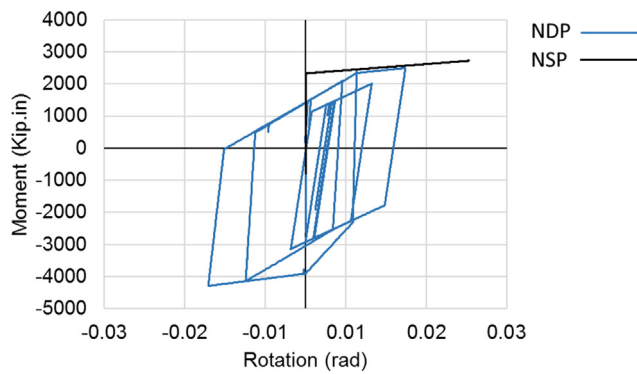


Fig. 12. Moment-rotation response of the left hinge of the beam shown in Fig. 11a for a single record in NDP (Imperial Valley EQ recorded at ElCentro) and the NSP results (1 kip = 4.448 kN, 1 in = 0.025 m). [The response for the NSP is terminated at the target displacement].

than the NDP results. In general, the inconsistency between the NDP and NSP is due to the inability of the fixed load distribution assumed in the NSP in predicting the demand distribution and specifically higher mode effects in the inelastic range of the response [22].

Various ground motion selection approaches may identify different ground motions for the same building at the same site as the target spectrum and/or selection criteria vary. The NDP results presented here for the archetype buildings are expected to change when a different ground motion selection approach is adopted. Analysis results for a set of similar steel moment frames show that the average  $DCR_N$  values computed using the ground motion selection approach adopted in this study are more conservative than the ones selected using the Conditional Mean Spectrum method (CMS) [23], but less conservative than the ground motions selected using the PEER toolbox [24].

### 5.5. Applicability of ASCE 41-17 and ASCE 7-16 to this study

ASCE 41-17 and ASCE 7-16 were published after the completion of this study. Although the underlying approaches of these standards are the same as their prior versions used in this study, *i.e.* ASCE 41-13 and ASCE 7-10, there are a few changes that can potentially impact the  $DCR_N$  values computed here for specific evaluation procedures. However, the general findings of this study are expected to be valid for the newer version of the standards. This section provides a discussion on the changes between the recent versions of ASCE 7 and 41, and the expected performance of ASCE 7-16 code-compliant RC moment frame buildings evaluated per ASCE 41-17. There are two main differences between ASCE 7-16 and 7-10 with regards to the design of the archetype RC moment frames considered in this study. The site coefficient value,  $F_v$ , is increased by 13%, for site class D, in ASCE 7-16 which can lead to a higher design base shear and, as a result, stronger and/or stiffer frames. In addition, the scaling of the base shear and drifts in the RSA design approach is increased from 85% to 100% of the ELF base shear and drift, respectively, in ASCE 7-16. This change would potentially lead to stronger and/or stiffer RSA-designed buildings.

In terms of the assessment of RC moment frames, the changes between the ASCE 41-13 and -17 can be divided into changes in the calculation of demand and capacity. ASCE 41-17 refers to ASCE 7-16 for calculation of the target response spectrum. As a result, the force demand calculated per ASCE 41-17 would increase proportionally to ASCE 7-16. In other words, the force demand used for the design, ASCE 7-16, and assessment, ASCE 41-17, both are increased with a similar

ratio in comparison with their prior editions. In terms of the calculation of the component capacity, m-factors, modeling parameters, and acceptance criteria for beams and beam-to-column joints did not change between the ASCE 41-17 and -13. In the linear procedure, the m-factors are slightly increased for the columns in the archetype buildings. In addition, the tensile axial force in columns is considered a deformation-controlled action in ASCE 41-17. The largest change between the two editions of ASCE 41 is the increase in the nonlinear modeling parameters and acceptance criteria for columns.

If the ELF-designed archetype frames are designed for ASCE 7-16 and assessed per ASCE 41-17, the increased demand in the design and assessment would be proportional. In the linear assessment, the slight increase in the m-factors of columns is expected to lead to slightly lower  $DCR_N$  values for columns, while the  $DCR_N$  of beams and joints would be the same. The  $DCR_N$  value of the corner columns calculated for tensile axial force is expected to be reduced because tension is considered a deformation-controlled action in ASCE 41-17. When nonlinear assessment procedures are employed, the changes in the modeling parameters and acceptance criteria of columns in ASCE 41-17 are expected to lead to lower  $DCR_N$  values for columns, and, as a result, more columns are expected to pass the ASCE 41 acceptance criteria. In the scenario the building is governed by a column story mechanism, ASCE 41-13 column modeling parameters may result in more concentrated deformations in columns at these levels due to a lower rotation at which peak strength is reached (“a” parameter in ASCE 41) relative to ASCE 41-17. As such, the story drifts would potentially be more uniform over the height of the building using the ASCE 41-17 modeling parameters, and higher demands on beams and joints may be found in other stories. In this case, the  $DCR_N$  values of beams and joints would increase as their acceptance criteria have not changed in ASCE 41-17. Please note that, in the current study all components of the archetype buildings passed the ASCE 41-13 acceptance criteria when NDP is employed with  $DCR_N$  values significantly less than 1.0. As a result, the use of the most recent version of the standards is not expected to change the findings of this study regarding the use of NDP.

Redesigning the RSA-designed archetype buildings per ASCE 7-16, would potentially lead to stronger and stiffer frames, due to the increase of the design base shear, that in turn lead to a better performance of the building when assessed using linear and nonlinear procedures in ASCE 41. Certainly, future studies should evaluate the expected performance of ASCE 7-16 code-compliant buildings based on the assessment requirements in ASCE 41-17.

It is worth mentioning that, although ASCE 7-16 and ASCE 41-16 are published, the IBC-15, which references ASCE 7-10, and IEBC-15, that references ASCE 41-13, are currently adopted by most states within the U.S. As a result, the ASCE 7-10 and ASCE 41-13 are still being used in practice, and the results of this study are applicable to the buildings that are being designed and evaluated in accordance with these standards.

## 6. Conclusion

A set of 4- and 8-story reinforced concrete special moment frames are designed in accordance with ASCE 7, and assessed using the four evaluation methodologies for Tier 3 analysis in ASCE 41, to study the correlation between the expected performances in these two standards. The assessment is conducted at the collapse prevention and life safety performance levels. The results show that the archetype buildings do not always pass the ASCE 41 acceptance criteria depending on the evaluation procedure employed and the performance level considered.

Analysis results show that linear procedures predict more conservative results than nonlinear procedures, for most components. At

the CP performance level and when LSP is used, columns in the first story of the all archetype buildings, as well as in the upper stories of the 8-story buildings, have  $DCR_N$  values between 1.01 and 6.5. For the LDP, all of the columns in the 4-story building showed a satisfactory performance. However, multiple columns over the height of the 8-story buildings reported  $DCR_N$  values between 1.05 and 4.0 at the CP performance level. The number of columns that did not pass the ASCE 41 acceptance criteria, was higher when LSP was employed as the evaluation methodology. The extent of failure of the columns in the upper stories of the 8-story RSA-designed building was more significant than the ELF-designed building at the CP performance level both in terms of number of components failed and the significance of the  $DCR_N$ . Beams in general performed better than columns.

At the LS performance level, the archetype buildings performed better and more components passed the ASCE 41 acceptance criteria. In the 4-story building, all components had  $DCR_N$  values less than one. For the 8-story ELF-designed building, only columns in the first story had  $DCR_N$  values greater than 1.0, with the maximum value of 1.86 when the LDP was employed. For the 8-story RSA-designed building, multiple columns over the height of the building had  $DCR_N$  greater than 1.0 with the maximum value of 2.34 for the interior columns. Results of linear procedures showed satisfactory performance per ASCE 41 for both joints and negative bending in the beams in all three buildings.

The difference between the predicted performance of the building's components using the linear evaluation procedure in ASCE 41 and design procedure in ASCE 7 is shown to be due to the differences in the calculation of component stiffness, gravity load, structure period, material properties, and how ductility is accounted for. The analysis results show that the discrepancy between the  $m$ - and  $j$ -factor in the assessment with the  $R$ -factor in the design procedure play the most important role in the inconsistency between the two standards. For the archetype moment frames in this study, the  $R$ -factor is up to four times greater than the  $m$ -factor. The analysis results show that the ELF-designed building tends to perform better than the RSA-designed building. This is believed to be a result of the higher base shear used in the design. To overcome this issue, ASCE 7-16 scales the RSA base shear design to 100% of the ELF design.

The analysis results revealed that consideration of column tension as a force-controlled action can be conservative and unrealistic, especially for corner columns. Moreover, further clarification in future cycles of ASCE 41 is needed on whether expected or nominal material properties should be used in developing the linear models or computation of the  $m$ -factors of various components.

The evaluation results for the nonlinear procedure showed that more components pass the acceptance criteria in comparison to the linear procedures. However, there are a few instances where the nonlinear static procedure produces the most conservative results for the beams. The results of the nonlinear static procedure also confirm the worse performance of the RSA-designed building in comparison with the ELF-designed building. At the CP performance level, all components with the exception of a few beams in the 4-story and 8-story RSA-designed buildings pass the acceptance criteria. At the LS performance level, all components meet the expected performance in ASCE 41 when NSP is employed. Among the four evaluation procedures, the nonlinear dynamic procedure is the only one for which all components of the

archetype buildings pass the ASCE 41 acceptance criteria with a large safety margin ratio.

The results of this study show that the four evaluation procedures in the Tier 3 analysis of ASCE 41 are not self-consistent and require further enhancement, especially with respect to the linear procedures. Assuming that NDP is the most accurate evaluation procedure, one could conclude that the  $m$ -factors used for modifying the capacity in the linear procedures are conservative and need to be revisited in future cycles of ASCE 41; if the values of the  $m$ - and  $R$ -factors were more similar then the discrepancy between ASCE 7 and ASCE 41 would be minimized. Moreover, the analysis results show that more components in the ASCE 7 code-compliant buildings satisfy the LS performance level targeted in ASCE 41. This observation implies a better agreement between the life safety performance level targeted by the two standards. It is noteworthy that some of the differences in the results of the linear and nonlinear procedures is due to the fact that nonlinear procedures in ASCE 41 use the acceptance criteria of the secondary components for the primary components, which is less conservative. However, the linear procedures distinguish between the  $m$ -factors of the primary and secondary components by introducing lower  $m$ -factors for primary components which leads to a more conservative assessment. This difference between the two approaches may need to be investigated further.

The findings of this study show that ASCE 7 and ASCE 41 are not consistent with respect to the expected performance of reinforced concrete special moment frames, which can potentially impact the resiliency of buildings in the same building community designed using loading, modeling, and analysis recommendations within the two standards. Future studies should evaluate the correlation between the performance targeted by ASCE 7-16 and ASCE 41-17 for RC moment frames. Moreover, whether ASCE 7 code-compliant buildings meet the 10% (or less) probability of collapse targeted by ASCE 7 for risk category II buildings need to be systematically investigated. The outcomes of this study illustrate the need for changes to the assessment and design standards provisions by building code developers if a consistent structural seismic performance is desired.

## Acknowledgments

The author gratefully acknowledges the contributions of Ms. Anne Hulsey in implementing the linear assessment procedure as well as Drs. Steven McCabe and John Harris for providing suggestions that greatly improved the manuscript.

## Disclaimer

Certain commercial software may have been used in the preparation of information contributing to this paper. Identification in this paper is not intended to imply recommendation or endorsement by NIST, nor is it intended to imply that such software is necessarily the best available for the purpose. Also, it is NIST policy to employ the International System of Units (metric units) in all of its publications. However, in the North American construction and building materials industries, certain non-SI units are used, therefore measurement values using both SI and customary units are included in this publication to avoid confusion.

## Appendix A

Tables A1 and A2.

**Table A1**  
Typical size and reinforcement of components in archetype buildings (1 in = 2.54 cm).

Story	# of stories Design method	4-story ELF/RSA				8-story ELF				8-story RSA			
		Frame		Interior		Exterior		Interior		Exterior		Interior	
		Spec.	Size (in)	Rebar	Size (in)	Rebar	Size (in)	Rebar	Size (in)	Rebar	Size (in)	Rebar	Size (in)
1st	Column	20 × 20	12#8	20 × 20	12#8	26 × 26	12#7	26 × 26	12#7	22 × 22	8#8	22 × 22	12#8
	E-W Beam	16 × 18	top:4#8 bot:3#7	16 × 18	top:4#8 bot:3#7	16 × 20	top:4#8 bot:3#8	16 × 20	top:4#8 bot:3#7	16 × 18	top:4#8 bot:3#8	16 × 18	top:4#8bot:3#8
2nd	Column	20 × 20	8#8	20 × 20	8#8	26 × 26	12#7	26 × 26	12#7	22 × 22	8#8	22 × 22	12#8
	E-W Beam	16 × 18	top:4#8 bot:3#7	16 × 18	top:4#8 bot:3#7	26 × 20	top:4#8 bot:3#8	26 × 20	top:4#8 bot:3#7	16 × 18	top:4#8 bot:3#8	16 × 18	top:4#8 bot:3#8
3rd	Column	20 × 20	8#8	20 × 20	8#8	26 × 26	12#7	26 × 26	12#7	22 × 22	8#8	22 × 22	12#8
	E-W Beam	16 × 18	top:3#8 bot:2#7	16 × 18	top:3#8 bot:2#7	16 × 20	top:4#8 bot:3#8	16 × 20	top:4#8 bot:3#7	16 × 18	top:4#8 bot:3#8	16 × 18	top:4#8 bot:3#8
4th	Column	20 × 20	8#7	20 × 20	8#7	24 × 24	12#7	24 × 24	12#7	22 × 22	8#8	20 × 20	12#8
	E-W Beam	16 × 18	top:3#7 bot:3#7	16 × 18	top:3#7 bot:2#7	16 × 20	top:4#8 bot:3#8	16 × 20	top:4#8 bot:3#7	16 × 18	top:4#8 bot:3#7	16 × 18	top:4#8 bot:3#8
5th	Column					24 × 24	12#7	24 × 24	12#7	22 × 22	8#8	20 × 20	12#8
	E-W Beam					16 × 20	top:4#8 bot:3#7	16 × 20	top:4#8 bot:3#7	16 × 16	top:4#8 bot:3#7	16 × 16	top:4#8 bot:3#7
6th	Column					20 × 20	12#7	20 × 20	12#7	18 × 18	8#8	18 × 18	8#9
	E-W Beam					16 × 18	top:4#8 bot:2#7	16 × 18	top:3#8 bot:2#7	16 × 16	top:4#8 bot:2#7	16 × 16	top:4#8 bot:2#7
7th	Column					20 × 20	12#7	20 × 20	12#7	18 × 18	8#7	18 × 18	8#9
	E-W Beam					16 × 18	top:3#8 bot:2#7	16 × 18	top:3#8 bot:2#7	16 × 16	top:3#8 bot:2#7	16 × 16	top:3#8 bot:2#7
8th	Column					20 × 20	12#7	20 × 20	12#7	18 × 18	8#7	18 × 18	8#7
	E-W Beam					16 × 18	top:3#7 bot:2#7	16 × 18	top:3#7 bot:2#7	16 × 16	top:3#8 bot:2#7	16 × 16	top:2#8 bot:2#7

**Table A2**  
Configuration of Rebars in U.S. customary and SI units.

Bar size	Nominal diameter (in)	Nominal diameter (mm)
#7	0.88	22.23
#8	1.00	25.4
#9	1.13	28.65

## References

- [1] FEMA. NEHRP guidelines for the seismic rehabilitation of buildings (FEMA 273). Washington D.C: Federal Emergency Management Agency; 1997.
- [2] FEMA. Prestandard and commentary for the seismic rehabilitation of buildings (FEMA 356). Federal Emergency Management Agency 2000.
- [3] ASCE/SEI. Seismic rehabilitation of existing buildings (ASCE/SEI 41-06). Reston, VA: American Society of Civil Engineers; 2006.
- [4] ASCE/SEI. Seismic rehabilitation of existing buildings (ASCE/SEI 41-13). Reston, VA: American Society of Civil Engineers; 2013.
- [5] Maison BF, Kasai K, Deierlein G. ASCE-41 and FEMA-351 evaluation of E-defense collapse test. *Earthq. Spectra* Nov. 2009;25(4):927–53.
- [6] Harris JH, Speicher MS. Assessment of first generation performance-based seismic design methods for new steel buildings, volume 1: special moment frames NIST-TN 1863-1 Gaithersburg, MD: NIST; 2015.
- [7] GSA. “Facilities Standards for the Public Buildings Service”. Washington D.C: U.S. General Services Administration; 2012.
- [8] ASCE/SEI. Minimum design loads for buildings and other structures (ASCE 7-10). Reston, Virginia: American Society of Civil Engineers; 2010.
- [9] Hagen GR. Performance-based analysis of a reinforced concrete shear wall building M.S. Thesis San Luis Obispo: California Polytechnic University; 2012.
- [10] Speicher MS, Harris JL. Collapse prevention seismic performance assessment of new eccentrically braced frames using ASCE 41. *Eng. Struct.* 2016;117:344–57.
- [11] Speicher MS, Harris JL. Collapse prevention seismic performance assessment of new special concentrically braced frames using ASCE 41. *Eng. Struct.* 2016;126:652–66.
- [12] ACI. ACI 318: building code requirements for reinforced concrete. Farmington Hills, MI; 2011.
- [13] Moehle JP, Hooper JD. Seismic design of reinforced concrete special moment frames: a guide for practicing engineers (NIST GCR-8-917-1) GCR-8-917-1 Gaithersburg, MD: National Institute of Standards and Technology; 2016.
- [14] CSI. ETABS user manual (v13.1.5). Berkeley, CA: Computer and Structures; 2013.
- [15] Siamak Sattar, Hulsey Anne M. Assessment of first generation performance-based seismic design methods: case study of a 4-story reinforced concrete special moment frame building. *Struct Congr* 2015.
- [16] CSI. PERFORM 3D user manual (v5.0.1). Berkeley, CA: Computer and Structures; 2011.
- [17] Sattar S, Liel AB. Collapse indicators for existing nonductile concrete frame buildings with varying column and frame characteristics. *Eng. Struct.* 2017;152:188–201.
- [18] Haselton CB, Liel AB, Deierlein GG, Chou J. Seismic collapse safety of reinforced concrete buildings. I: Assessment of ductile moment frames read more: [http://ascelibrary.org/doi/abs/10.1061/\(ASCE\)ST.1943-541X.0000318](http://ascelibrary.org/doi/abs/10.1061/(ASCE)ST.1943-541X.0000318). *J. Struct. Eng.* 2011;37(4):481–91.
- [19] ATC. Modeling and acceptance criteria for seismic design and analysis of tall buildings. Redwood City, CA: Applied Technology Council, PEER 2010/111; 2010.
- [20] Matamoros A. Study of drift limits for high-strength concrete columns. Champaign: University of Illinois at Urbana-Champaign; 1999.
- [21] FEMA. Quantification of building seismic performance factors (FEMA P695). Redwood City, CA: Applied Technology Council; 2009.
- [22] Mwafy AM, Elnashai AS. Static pushover versus dynamic collapse analysis of RC buildings. *Eng. Struct.* 2001;23(5):407–24.
- [23] Baker JW. Conditional mean spectrum: tool for ground-motion selection. *J. Struct. Eng.* 2011;137(3):322–31.
- [24] Uribe R, Sattar S, Speicher MS, Ibarra L. Influence of ground motion selection on the assessment of steel moment frames. In: 16WCEE, Santiago, Chile; 2016.